Journal of Siberian Federal University. Chemistry 3 (2010 3) 207-215
~ ~ ~

УДК 546

Carbon Monoxide Disproportionation over Ceria-Containing Materials

Meghan E. Swanson, Vladimir V. Pushkarev, Vladimir I. Kovalchuk* and Julie L. d'Itri
Department of Chemical Engineering, University of Pittsburgh, Pittsburgh, Pennsylvania 15261 [1]

Received 6.09.2010, received in revised form 13.09.2010, accepted 20.09.2010

The disproportionation of CO catalyzed by ceria is demonstrated in this Raman spectroscopic investigation of the interaction of CO with ZrO_2, Pd/ZrO_2, $Ce_{0.75}Zr_{0.25}O_2$, and $Pd/Ce_{0.75}Zr_{0.25}O_2$

Keywords: disproportionation, carbon monoxide, ceria, zirconia, Raman spectroscopy

Introduction

The disproportionation of CO to carbon and CO_2 is favored thermodynamically at temperatures less than 1000 K; however, the gas phase reaction kinetics are extremely slow [1]. Metals such as Ni [2-6], Fe [7, 8], Co [4, 8, 9], Pt [10], Pd [11-13], Ru [14], and Rh [15] readily catalyze the reaction. And it has also been reported that CO disproportionation is facile on metal oxides such as MgO [16] and Fe_3O_4 [17]; albeit these metal oxides are considered as less active catalysts than the metals.

Based on FTIR investigations of the surface species formed upon exposure to CO, Li et al. inferred CeO_2 catalyzes CO disproportionation [18]. A recent Raman study also provided results consistent with CO disproportionation catalyzed by CeO_2 [19, 20]. The propensity of ceria-based materials to catalyze CO disproportionation is important to understand because CeO_2 is used in automotive catalytic converters as an oxygen buffer and the oxygen buffering capacity of the catalyst is measured using the assumption of stoichiometric oxidation of CO [21].

The objective of this research was to provide unambiguous evidence whether or not CeO_2 catalyzes CO disproportionation. Specifically, experiments were conducted with $Ce_{0.75}Zr_{0.25}O_2$ and ZrO_2, both as pure materials and with deposited Pd metal, and the results were compared to the reported Raman bands at 1582 and 1331 cm^{-1} observed after CeO_2 is exposed to CO [19,20]. Zirconia is not expected to catalyze the reaction and was used as a reference material, yet, it has been suggested that ceria is active for CO disproportionation [18-20]. The Raman spectra obtained for the two oxides were compared to spectra obtained for the 1% Pd-supported oxides for purposes of delineating between CO disproportionation catalysis by the metal oxide and the metal [11-13].

* Corresponding author E-mail address: vkovalch@gmail.com

Experimental

Zirconia was precipitated from an aqueous solution of $ZrO(NO_3)_2$ (Alfa, 99.9%) with aqueous ammonia at pH 10. The precipitate was aged in the supernatant liquid for 24 h before filtering, washing, and drying at 373 K for 12 h; it was then calcined in air at 773 K for 12 h. The ceria-zirconia ($Ce_{0.75}Zr_{0.25}O_2$, 99.9%) was supplied by Rhodia, and it was calcined in air at 823 K for 12 h. The 1% Pd supported catalysts were prepared by impregnation of ZrO_2 and $Ce_{0.75}Zr_{0.25}O_2$ with aqueous solutions of $Pd(NH_3)_4(NO_3)_2$ (Strem Chemicals, 99.9%). The impregnated samples were dried at 373 K for 12 h and then calcined in air at 823 K for 12 h.

After calcination, the specific surface area, pore volume distribution, and average pore diameter of the materials were obtained from N_2 physisorption data acquired using a Micromeritics (ASAP 2010) volumetric sorption analyzer. The catalysts were degassed by evacuation for 2 h at 673 K prior to the measurements, and these characterization results are shown in Table 1.

The Raman spectra were obtained using a Renishaw System 2000 Raman spectrometer equipped with a Leica DMLM microscope and a 514.5-nm Ar^+ ion laser as the excitation source. The laser power at the source was 5-25 mW, which caused minimal sample damage [22]. An Olympus x50 objective was used to focus the unpolarized laser beam onto a <3 μm spot on the sample, and to collect the backscattered light. Ten scans, each at a resolution of 4 cm^{-1}, were collected for each spectrum in the 100-4000 cm^{-1} range. The *in-situ* Raman measurements were conducted at atmospheric pressure in a THMS 600 Raman cell from Linkam Scientific. Approximately 100 mg of the catalyst was pressed into a 10 mm pellet, which was then mounted in the *in-situ* cell.

The He (Air Products, >99.998%) and CO (Praxair, >99.995%) were scrubbed of water and oxygen impurities using zeolite and OxyTrap filters, both from Alltech. The CO was fitted with an additional trap, Vista B γ-alumina heated to 573 K, to remove metal carbonyl contaminants. The 10% O_2 in He (Praxair, UHP) was used without further purification. The reaction gases (CO, He, and 10% O_2/He) were mixed prior to the Raman cell, and the desired flow rate of each gas was maintained within ± 1 cm^3/min using Brooks mass flow controllers (model 5850E). The total gas flow rate was 100 cm^3/min for all treatments and experiments, and the heating or cooling rate was always 10 K/min.

The sample pretreatment consisted of heating the sample from room temperature to 673 K in 10% CO/He, and maintaining these conditions for 1 h. Subsequently, the gas flow was changed to 10% O_2/He at 673 K for 1 h. Then, the sample was cooled to 623 K in 10% O_2/He, a spectrum was taken, and the cell was purged with He for 15 min at 623 K. Next, the gas flow was switched to 10% CO/He for 1 h and then a spectrum was recorded.

Table 1. Catalyst textural properties

Material	Surface area (m^2/g)	Pore volume (cm^3/g)	Average Pore diameter (nm)
ZrO_2	51	0.117	7.5
$Ce_{0.75}Zr_{0.25}O_2$	106	0.287	9.3
1% Pd/ZrO_2	49	0.103	8.0
1% Pd/$Ce_{0.75}Zr_{0.25}O_2$	114	0.288	9.0

Results and Discussion

The Raman spectrum of ZrO_2 at 623 K in 10% O_2/He exhibited one band in the hydroxyl region at 3667 cm^{-1} (Fig. 1a). Subsequent exposure of the sample to CO at 623 K for 1 h resulted in the appearance of four new bands: 1385, 1561, 2872, and 2979 cm^{-1} (Fig. 1b). The four band positions are consistent with an assignment of surface formate species. The bands at 1561 cm^{-1} and 1385 cm^{-1} are assigned to the C-H bending and O-C-O stretching vibrations [23-25], respectively. The 2872 cm^{-1} band is attributed to the formate C-H stretch [23-25], and the 2979 cm^{-1} band is assigned to a combination [23-25] of the 1561 and 1385 cm^{-1} bands [26]. The spectrum of Pd/ZrO_2 at 623K after 1 h exposure to CO contained only bands at 1582 cm^{-1} and 1331 cm^{-1} (Fig. 1d). No hydroxyl band was detected; however, the band(s) may be obscured by the strong fluorescence in the region of 2000-4000 cm^{-1}.

With $Ce_{0.75}Zr_{0.25}O_2$ at 623 K in 10% O_2/He, two bands were observed (Fig. 2a). One band, at 3654 cm^{-1}, is in the hydroxyl region. The other band at 1206 cm^{-1} is consistent with the oxide lattice vibrations. Prior Raman studies of $Ce_xZr_{1-x}O_2$ did not present spectra above 1000 cm^{-1} [27-30]. However, CeO_2 exhibits a band at 1166 cm^{-1} that is assigned to a combination of the A_{1g}, E_g, and F_{2g} vibrational modes of the ceria lattice [31], and both the CeO_2 and the $Ce_xZr_{1-x}O_2$ have a cubic fluorite crystal structure [32]. One would expect that the 1166 cm^{-1} lattice vibration of CeO_2 shifted to 1206 cm^{-1} in $Ce_{0.75}Zr_{0.25}O_2$ because the smaller ionic radius of the Zr

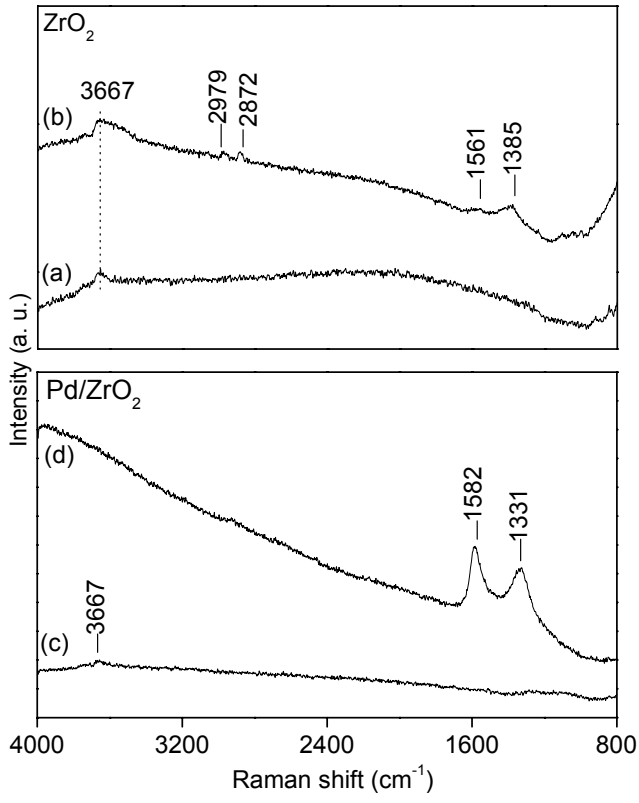

Fig. 1. Top: *In situ* Raman spectra of ZrO_2 (a) after pretreatment in 10% O_2/He at 673 K for 1 h and (b) after subsequent exposure to 10% CO/He at 623 K for 1 h. Bottom: *In situ* Raman spectra of 1% Pd/ZrO_2 (c) after pretreatment in 10% O_2/He at 673 K for 1 h and (d) after subsequent exposure to 10% CO/He at 623 K for 1 h. All spectra were recorded at 623 K

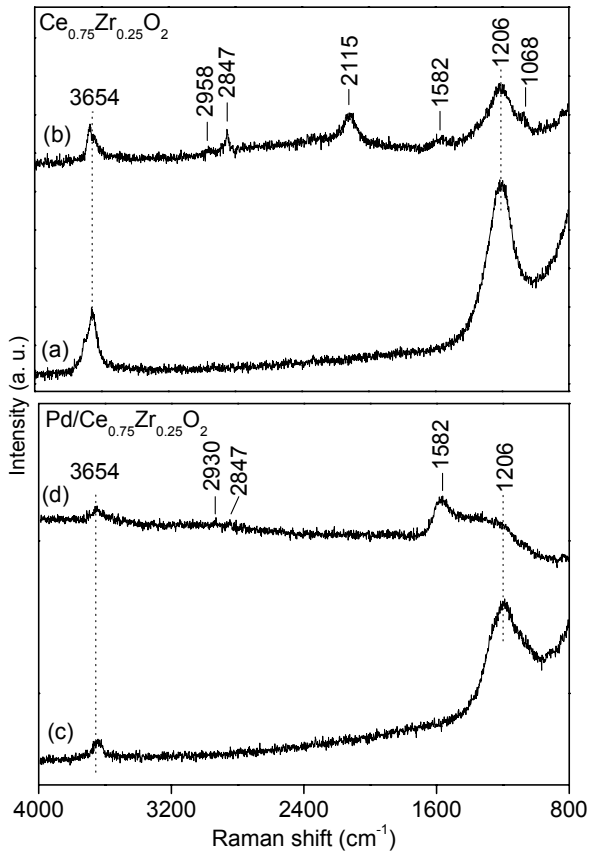

Fig. 2. Top: *In situ* Raman spectra of $Ce_{0.75}Zr_{0.25}O_2$ (a) after pretreatment in 10% O_2/He at 673 K for 1 h and (b) after subsequent exposure to 10% CO/He at 623 K for 1 h. Bottom: *In situ* Raman spectra of 1% $Pd/Ce_{0.75}Zr_{0.25}O_2$ (c) after pretreatment in 10% O_2/He at 673 K for 1 h and (d) after subsequent exposure to 10% CO/He at 623 K for 1 h. All spectra were recorded at 623 K

cations, compared to the Ce cations, results in a contraction of the lattice [32-33]. Such a lattice contraction manifests itself in the Raman spectra as a shift of the lattice vibrational bands to higher wavenumbers [34-35].

Exposure of the $Ce_{0.75}Zr_{0.25}O_2$ to CO resulted in the appearance of four new bands: 2847, 2115, 1582, and 1068 cm^{-1} (Fig. 2b). The presence of a low intensity band at 2958 cm^{-1} cannot be ruled out despite the poor signal to noise ratio. As well, a low intensity band at 1331 cm^{-1} cannot be ruled out because it may be obscured by the broad band at 1206 cm^{-1}. In accordance with the band assignment for ZrO_2, the 2958 and 2847 cm^{-1} bands observed with $Ce_{0.75}Zr_{0.25}O_2$ are attributed to formate species [26]. The band at 1068 cm^{-1} has been assigned to carbonate species [36-40]. Several earlier investigations concluded the 2115 cm^{-1} band is characteristic of Ce^{3+} species. In one study the band was assigned to the CO stretching mode of CO-Ce^{3+} [41], and in two other studies it was assigned to the symmetry-forbidden $^2F_{5/2} \rightarrow {}^2F_{7/2}$ electronic transition of Ce^{3+} [37,39].

The bands observed with $Pd/Ce_{0.75}Zr_{0.25}O_2$ at 623 K in 10% O_2/He were similar to those obtained with $Ce_{0.75}Zr_{0.25}O_2$ under the same condition: a hydroxyl vibration at 3654 cm^{-1} and a lattice vibration at 1206 cm^{-1} (Fig. 2c). After exposure of $Pd/Ce_{0.75}Zr_{0.25}O_2$ to CO at 623 K for 1 h, a distinct band appeared at 1582 cm^{-1}, with a shoulder peak in the vicinity of 1331 cm^{-1} (Fig. 2d). As well, formate bands at 2930 and 2847

cm^{-1} were observed, which in not surprising for zirconia-containing materials; such species have been reported to be stable at high temperatures [42-43].

The most exciting result of this investigation is the presence of a band at 1582 cm^{-1} after exposure of $Ce_{0.75}Zr_{0.25}O_2$ to CO at 623 K. The band position is inconsistent with formate species on metal free ZrO_2 (Fig. 1b), and the band cannot be attributed to a formate species on ceria. In addition, only traces of formates have been detected on ceria exposed to CO after oxidation; however, appreciable amounts of formates have been reported for ceria pre-reduced with H_2 prior to CO exposure [44-45]. Rather, cerium carbonates and/or carboxylates form after pre-oxidation and subsequent exposure to CO [38,39,45]. As well, the band cannot be assigned to zirconium carbonates/carboxylates, as they are thermally unstable at 623 K [42-43]. However, a Raman band at 1582 cm^{-1} has been reported for CeO_2 exposed to CO after pre-oxidation with O_2 [19-20]. Moreover, this investigation reports the presence of a Raman band at 1582 cm^{-1} for both $Pd/Ce_{0.75}Zr_{0.25}O_2$ and Pd/ZrO_2 exposed to CO after pre-oxidation (Fig. 1, 2).

The bands at 1582 and 1331 cm^{-1} observed with Pd/ZrO_2, $Ce_{0.75}Zr_{0.25}O_2$, and $Pd/Ce_{0.75}Zr_{0.25}O_2$ after exposure to CO (Figures 1,2) are in the same position as the bands tentatively assigned to carbonaceous deposits on CeO_2 [19-20] upon exposure to CO after pre-oxidation [46-54]. Graphite and other sp^2-hybridized carbons exhibit strong Raman bands in these positions – namely, there is a Raman active E_{2g} carbon-carbon stretching mode at 1582 cm^{-1} [46-52], and a Raman active breathing mode of a sp^2-hybridized carbon with A_{1g} symmetry in the vicinity of 1331 cm^{-1} [48-51,53,54]. The A_{1g} breathing mode is forbidden in large perfect crystals, but becomes Raman active in small crystallites [48-51,53,54].

Conclusion

It has been demonstrated that CO disproportionates on CeO_2 and ceria-based mixed oxides at conditions of industrial significance. With Pd/ZrO_2 the bands at 1582 and 1331 cm^{-1} are the result of carbon formed via the CO disproportionation on Pd; these bands are not observed with ZrO_2 under the same conditions. Bands in the same positions are observed with $Ce_{0.75}Zr_{0.25}O_2$ after exposure to CO at 623 K – clear evidence that these metal oxides catalyze carbon formation via a CO disproportionation route.

Acknowledgements

Support from the Petroleum Research Fund (grant No PRF 39801 AC5S) of the American Chemical Society and National Science Foundation (CTS 0086638) is gratefully acknowledged.

References

1. Cheng, H.; Reiser, D. B.; Dean, S., Jr., On the mechanism and energetics of Boudouard reaction at FeO(100) surface $2CO \rightarrow C+CO_2$. *Catal. Today* **1999,** 50, (3-4), 579-587.

2. Nakano, H.; Kawakami, S.; Fujitani, T.; Nakamura, J., Carbon deposition by disproportionation of CO on a Ni(977) surface. *Surf. Sci.* **2000,** 454-456, 295-299.

3. Martra, G.; Marchese, L.; Arena, F.; Parmaliana, A.; Coluccia, S., Surface structure of Ni/MgO catalysts: effects of carbon and hydrogen on the reactivity towards CO. HRTEM and FTIR studies. *Top. Catal.* **1994,** 1, (1,2), 63-73.

4. Highfield, J. G.; Bossi, A.; Stone, F. S., Dispersed-metal/oxide catalysts prepared by reduction of high surface area oxide solid solutions. *Stud. Surf. Sci. Catal.* **1983,** 16, 181-92.

5. Govindaraj, A.; Sen, R.; Santra, A. K.; Nagaraju, B. V., Carbon structures obtained by the disproportionation of carbon monoxide over nickel catalysts. *Mater. Res. Bull.* **1998,** 33, (4), 663-667.

6. Guinot, J.; Audier, M.; Coulon, M.; Bonnetain, L., Formation and characterization of catalytic carbons obtained from carbon monoxide disproportionation over an iron-nickel catalyst. I. Fragmentation and rates of carbon deposition. *Carbon* **1981,** 19, (2), 95-98.

7. Geurts, F. W. A. H.; Sacco, A., Jr., The relative rates of the Boudouard reaction and hydrogenation of carbon monoxide over iron and cobalt foils. *Carbon* **1992,** 30, (3), 415-418.

8. Moeller, P.; Papp, H., Heats of adsorption and reaction of carbon monoxide on iron/manganese oxide catalysts. *Adsorpt. Sci. Technol.* **1987,** 4, (3), 176-184.

9. Nakamura, J.; Tanaka, K.; Toyoshima, I., Reactivity of deposited carbon on cobalt-alumina catalyst. *J. Catal.* **1987,** 108, (1), 55-62.

10. Gavril, D.; Koliadima, A.; Karaiskakis, G., Adsorption Studies of Gases on Pt-Rh Bimetallic Catalysts by Reversed-Flow Gas Chromatography. *Langmuir* **1999,** 15, (11), 3798-3806.

11. Ichikawa, S.; Poppa, H.; Boudart, M., The effect of particle size on the reactivity of supported palladium. *ACS Symp. Ser.* **1984,** 248 (Catal. Mater.: Relat. Struct. React.), 439-451.

12. Matolin, V.; Gillet, E., Carbon monoxide disproportionation over supported palladium particles: a TPD and static SIMS study. *Surf. Sci.* **1990,** 238, (1-3), 75-82.

13. Gredig, S.; Tagliaferri, M.; Maciejewski, M.; Baiker, A., Oxidation and disproportionation of carbon monoxide over Pd/ZrO2 catalysts prepared from glassy Pd-Zr alloy and by co-precipitation. *Stud. Surf. Sci. Catal.* **1995,** 96, 285-294.

14. Yokomizo, G. H.; Louis, C.; Bell, A. T., Thermal desorption and disproportionation of carbon monoxide adsorbed on ruthenium/silica. *J. Catal.* **1989,** 120, (1), 15-21.

15. Orita, H.; Naito, S.; Tamaru, K., Reactivity of surface carbon deposited on supported rhodium catalysts by the disproportionation of carbon monoxide. *J. Catal.* **1988,** 111, (2), 464-467.

16. Zecchina, A.; Coluccia, S.; Spoto, G.; Scarano, D.; Marchese, L., Revisiting magnesium oxide-carbon monoxide surface chemistry: an IR investigation. *J. Chem. Soc., Faraday Trans.* **1990,** 86, (4), 703-709.

17. Watanabe, M.; Kadowaki, T., Dissociation reactions of CO gas on Fe and Fe_3O_4 surfaces observed by Raman-ellipsometry spectroscopy. *Appl. Surf. Sci.* **1987,** 28, (2), 147-166.

18. Li, C.; Sakata, Y.; Arai, T.; Domen, K.; Maruya, K.; Onishi, T., Carbon monoxide disproportionation at mild temperatures over partially reduced cerium oxide. *J. Chem. Soc., Chem. Commun.* **1991**, (6), 410-411.

19. Swanson, M.; Pushkarev, V. V.; Kovalchuk, V. I.; d'Itri, J. L., The dynamic surface chemistry during the interaction of CO with ceria captured by Raman spectroscopy. *Catal. Lett.* **2007,** 116, (1-2), 41-45.

20. Swanson, M.; Pushkarev, V. V.; Kovalchuk, V. I.; d'Itri, J. L., Evidence for CO Disproportionation over Ceria during Oxygen Storage Capacity Measurements: An in Situ Raman Spectroscopic Investigation. *J. Siber. Federal Univ. Chem.* **2008,** 1, (1), 24-34.

21. Yao, H.; Yu Yao, Y., Ceria in automotive exhaust catalysts 1. Oxygen storage. *J. Catal.* **1984,** 86, (2), 254-265.

22. Pushkarev, V. V.; Kovalchuk, V. I.; d'Itri, J. L., Probing Defect Sites on the CeO_2 Surface with Dioxygen. *J. Phys. Chem. B* **2004,** 108, (17), 5341-5348.

23. Mugniery, X.; Chafik, T.; Primet, M.; Bianchi, D., Characterization of the sites involved in the adsorption of CO on ZrO_2 and ZnO/ZrO_2 methanol synthesis aerogel catalysts. *Catal. Today* **1999,** 52, (1), 15-22.

24. Bianchi, D.; Chafik, T.; Khalfallah, M.; Teichner, S. J., Intermediate species on zirconia supported methanol aerogel catalysts. II. Adsorption of CO on pure zirconia and on zirconia containing zinc oxide. *App. Catal., A* **1993,** 105, (2), 223-249.

25. Kalies, H.; Pinto, N.; Pajonk, G. M.; Bianchi, D., Hydrogenation of formate species formed by CO chemisorption on a zirconia aerogel in the presence of platinum. *Appl. Catal., A* **2000,** 202, (2), 197-205.

26. Li, C.; Domen, K.; Maruya, K.; Onishi, T., Spectroscopic identification of adsorbed species derived from adsorption and decomposition of formic acid, methanol, and formaldehyde on cerium oxide. *J. Catal.* **1990,** 125, (2), 445-455.

27. Yashima, M.; Arashi, H.; Kakihana, M.; Yoshimura, M., Raman Scattering Study of Cubic-Tetragonal Phase Transition in $Zr_{1-x}Ce_xO_2$ Solid Solution. *J. Am. Ceram. Soc.* **1994,** 77, (4), 1067-1071.

28. Reddy, B. M.; Khan, A.; Lakshmanan, P.; Aouine, M.; Loridant, S.; Volta, J.-C., Structural Characterization of Nanosized CeO_2-SiO_2, CeO_2-TiO_2, and CeO_2-ZrO_2 Catalysts by XRD, Raman, and HREM Techniques. *J. Phys. Chem. B* **2005,** 109, (8), 3355-3363.

29. Fornasiero, P.; Spenghini, A.; Di Monte, R.; Bettinelli, M.; Kaspar, J.; Bigotto, A.; Sergo, V.; Graziani, M., Laser Excited Luminescence of Trivalent lanthanide Impurities and Local Structure in CeO_2-ZrO_2 Mixed Oxides. *Chem. Mater.* **2004,** 16, (10), 1938-1944.

30. Vlaic, G.; Di Monte, R.; Fornasiero, P.; Fonda, E.; Kaspar, J.; Graziani, M., Redox Property-Local Structure Relationships in the Rh-Loaded CeO_2-ZrO_2 Mixed Oxides. *J. Catal.* **1999,** 182, (2), 378-389.

31. Weber, W.; Hass, K.; McBride, J., Raman study of CeO_2: second-order scattering, lattice dynamics, and particle-size effects. *Phys. Rev. B* **1993,** 48, (1), 178-185.

32. Deshmukh, S. S.; Zhang, M.; Kovalchuk, V. I.; d'Itri, J. L., Effect of SO_2 on CO and C_3H_6 oxidation over CeO_2 and $Ce_{0.75}Zr_{0.25}O_2$. *App. Catal., B* **2003,** 45, (2), 135-145.

33. Fornasiero, P.; DiMonte, R.; Ranga Rao, G.; Kaspar, J.; Meriani, S.; Trovarelli, A.; Graziani, M., Rh-loaded CeO_2-ZrO_2 Solid solutions as highly effective oxygen exchangers: dependence on the reduction behavior and the OSC on the structural properties. *J. Catal.* **1995,** 151, (1), 168-177.

34. Ichikawa, S.; Suda, J.; Sato, T.; Suzuki, Y., Lattice dynamics and temperature dependence of the first-order Raman spectra for α-SiO_2 crystals. *J. Raman Spectrosc.* **2003,** 34, (2), 135-141.

35. Bertheville, B.; Bill, H., The temperature dependence of the Raman T_{2g} lattice mode in K_2S crystals. *Solid State Ionics* **2001,** 139, (1,2), 159-162.

36. Laachir, A.; Perrichon, V.; Badri, A.; Lamotte, J.; Catherine, E.; Lavalley, J. C.; El Fallah, J.; Hilaire, L.; Le Normand, F., Reduction of cerium dioxide by hydrogen. Magnetic susceptibility and Fourier-transform infrared, ultraviolet and x-ray photoelectron spectroscopy measurements. *J. Chem. Soc., Faraday Trans.* **1991,** 87, (10), 1601-1609.

37. Binet, C.; Badri, A.; Lavalley, J.-C., A Spectroscopic Characterization of the Reduction of Ceria from Electronic Transitions of Intrinsic Point Defects. *J. Phys. Chem.* **1994,** 98, (25), 6392-6398.

38. Li, C.; Sakata, Y.; Arai, T.; Domen, K.; Maruya, K.; Onishi, T., Carbon monoxide and carbon dioxide adsorption on cerium oxide studied by Fourier-transform infrared spectroscopy. 1. Formation of carbonate species on dehydroxylated cerium dioxide at room temperature. *J. Chem. Soc., Faraday Trans. 1* **1989,** 85, (4), 929-943.

39. Bozon-Verduraz, F.; Bensalem, A., IR studies of cerium dioxide: influence of impurities and defects. *J. Chem. Soc., Faraday Trans.* **1994,** 90, (4), 653-657.

40. Binet, C.; Badri, A.; Boutonnet-Kizling, M.; Lavalley, J. C., FTIR study of carbon monoxide adsorption on ceria: CO_2^{2-} carbonite dianion adsorbed species. *J. Chem. Soc., Faraday Trans.* **1994,** 90, (7), 1023-1028.

41. Bensalem, A.; Muller, J.-C.; Tessier, D.; Bozon-Verduraz, F., Spectroscopic study of CO adsorption on palladium-ceria catalysts. *J. Chem. Soc., Faraday Trans.* **1996,** 92, (17), 3233-3237.

42. Fisher, I. A.; Bell, A. T., In situ infrared study of methanol synthesis from H_2/CO over Cu/SiO_2 and Cu/ZrO_2/SiO_2. *J. Catal.* **1998,** 178, (1), 153-173.

43. Pokrovski, K.; Jung, K. T.; Bell, A. T., Investigation of CO and CO_2 adsorption on tetragonal and monoclinic zirconia. *Langmuir* **2001,** 17, (14), 4297-4303.

44. Li, C.; Sakata, Y.; Arai, T.; Domen, K.; Maruya, K.; Onishi, T., Adsorption of carbon monoxide and carbon dioxide on cerium oxide studied by Fourier-transform infrared spectroscopy. 2. Formation of formate species on partially reduced cerium dioxide at room temperature. *J. Chem. Soc., Faraday Trans. 1* **1989,** 85, (6), 1451-1461.

45. Binet, C.; Jadi, A.; Lavalley, J. C., IR study of carbon dioxide and carbon monoxide adsorption onto ceria- effect of the reduction state of ceria. *J. Chim. Phys. Phys.-Chim. Biol.* **1992,** 89, (9), 1779-1797.

46. Wang, Y.; Alsmeyer, D. C.; McCreery, R. L., Raman spectroscopy of carbon materials: structural basis of observed spectra. *Chem. Mater.* **1990,** 2, (5), 557-563.

47. Dillon, R. O.; Woollam, J. A.,; Katkanant, V., Use of Raman scattering to investigate disorder and crystallite formation in as-deposited and annealed carbon films. *Phys. Rev. B* **1984,** 29, (6), 3482-3489.

48. Nemanich, R. J.; Solin, S. A., First- and second-order Raman scattering from finite-size crystals of graphite *Phys. Rev. B* **1979,** 20, (2), 392-401.

49. Nathan, M. I.; Smith, J. E.; Tu, K. N., Raman spectrum of glassy carbon. *J. Appl. Phys.* **1974,** 45, (5), 2370-2371.

50. Tuinstra, F.; Koenig, J. L., Raman spectrum of graphite. *J. Chem. Phys.* **1970,** 53, (3), 1126-1130.

51. Knight, D. S.; White, W. B., Characterization of diamond films by Raman spectroscopy. *J. Mater. Res.* **1989,** 4, (2), 385-393.

52. Al-Jishi, R.; Dresselhaus, G., Lattice-dynamical model for graphite. *Phys. Rev. B* **1982,** 26, (8), 4514-4522.

53. Matthews, M. J.; Pimenta, M. A.; Dresselhaus, G.; Dresselhaus, M. S.; Endo, M., Origin of the dispersive effects of the Raman D band in carbon materials. *Phys. Rev. B* **1999,** 59, (10), R6585-R6588.

54. Poscik, I.; Hundhausen, M.; Koos, M.; Ley, L., Origin of the D peak in the Raman spectrum of microcrystalline graphite. *J. Non-Cryst. Solids* **1998,** 227-230, (2), 1083-1086.

Диспропорционирование моноксида углерода на катализаторах, содержащих оксид церия

М.Е. Свансон, В.В. Пушкарёв,
В.И. Ковальчук, Дж.Л. д'Итри
Департамент химической технологии, Питсбургский университет
Питсбург, Пенсильвания 15261

Методом спектроскопии комбинационного рассеяния исследовано взаимодействие CO с ZrO_2, Pd/ZrO_2, $Ce_{0.75}Zr_{0.25}O_2$ и $Pd/Ce_{0.75}Zr_{0.25}O_2$ катализаторами дожигания выхлопных газов. Показана возможность диспропорционирования моноксида углерода в условиях измерения буферной ёмкости каталитических материалов по кислороду.

Ключевые слова: реакция Будуара, моноксид углерода, оксид церия, оксид циркония, Рамановская спектроскопия.